

ResearchSpace@Auckland

Version

This is the Accepted Manuscript version. This version is defined in the NISO recommended practice RP-8-2008 <http://www.niso.org/publications/rp/>

Suggested Reference

Hermann, S., Morales, S., & Klette, R. (2011). Half-Resolution Semi-Global Stereo Matching. In *IEEE Intelligent Vehicles Symposium, Proceedings* (pp. 201-206). Baden-Baden, GERMANY: IEEE. doi: [10.1109/IVS.2011.5940427](https://doi.org/10.1109/IVS.2011.5940427)

Copyright

Items in ResearchSpace are protected by copyright, with all rights reserved, unless otherwise indicated. Previously published items are made available in accordance with the copyright policy of the publisher.

© 2011 IEEE. Personal use of this material is permitted. Permission from IEEE must be obtained for all other uses, in any current or future media, including reprinting/republishing this material for advertising or promotional purposes, creating new collective works, for resale or redistribution to servers or lists, or reuse of any copyrighted component of this work in other works.

http://www.ieee.org/publications_standards/publications/rights/rights_policies.html

<https://researchspace.auckland.ac.nz/docs/uoa-docs/rights.htm>

Half-Resolution Semi-Global Stereo Matching

Simon Hermann, Sandino Morales and Reinhard Klette

.enpeda.. group, Department of Computer Science, University of Auckland, New Zealand

Abstract—Semi-global matching is a popular choice for applications where dense and robust stereo estimation is required and real-time performance is crucial. It therefore plays an important role in vision-based driver assistance systems. The strength of the algorithm comes from the integration of multiple 1D energy paths which are minimized along eight different directions across the image domain. The contribution of this paper is twofold. First, a thorough evaluation of stereo matching quality is performed when the number of accumulation paths is reduced. Second, an alteration of semi-global matching is proposed that operates only on half of the image domain without losing disparity resolution. The evaluation is performed on four real-world driving sequences of 400 frames each, as well as on 396 frames of a synthetic image sequence where sub-pixel accurate ground truth is available. Results indicate that a reduction of accumulation paths is a very good option to improve the run-time performance without losing significant quality, even on sub-pixel level. Furthermore, operating semi-global matching only on half the image yields almost identical results to the corresponding full path integration. This approach yields the potential to further speed up the runtime and could also be exploited for other alterations of the algorithm.

I. INTRODUCTION AND RELATED LITERATURE

Stereo estimation by semi-global matching (SGM) [1] is popular for industrial applications where dense and robust real-time stereo matching is required for high frame rates, for example of 30 Hz in current vision-based *driver assistance systems* (DAS). Recently a Daimler AG research group presented their design of an FPGA implementation [2] that reaches this frame rate running on eight accumulation paths. Other authors announced a close to real-time GPU based implementation [3] for images of size 640×480 . The original paper by Heiko Hirschmüller [1] recommended the use of 16 (and at least 8) paths for data accumulation to achieve high quality results. The stereo community in general follows this recommendation and uses eight paths.

The major constraint in the design of a real-time SGM implementation is the available memory throughput in current hardware. Because SGM integrates along 1D energy paths in multiple directions, a large memory block needs to be updated in off-chip memory. Depending on the implementation design, reducing accumulation directions reduces the memory access and can lead to a significant run-time improvement in SGM [5]. In our previous study [4] a first attempt was made to test the change in stereo quality when costs are accumulated only along four paths. Unfortunately, the evaluation was performed on one data set only and

the result is therefore not representative. Another group [5] reported to work with a GPU implementation of SGM that processes at least 24 fps. They reach this frame rate by omitting the diagonal integration paths and therefore omitting 50% of the accumulations. They showed by example and discussion that the quality decrease on their stereo sequences is only marginal compared to the significant run-time improvement. However, they did not quantify the performance loss for ensuring this run-time gain. To our best knowledge, no study so far thoroughly evaluates traffic sequences to quantify the performance loss that results when integrating along four instead of eight paths. This study aims to close this gap and quantifies the tradeoff in performance that comes with a faster execution of SGM. Furthermore, it is proposed to perform SGM integration on only half of the image resolution to yield faster execution by changing the algorithm design of the accumulation step. Note, that calculating stereo maps on half-resolution stereo image pairs has already been done in [2]. However, the major contribution in our proposal is, to keep the full disparity resolution and not to reduce the maximum disparity by factor 2.

The outline of this paper is as follows. In Section II, relevant details of the SGM algorithm are recalled and parameter settings of the used implementation are given. Section III presents the different integration strategies which are evaluated. This includes the reduction of accumulation directions from eight to four paths (along the image axes), as well as a possible further reduction down to two paths. The latter strategy is designed such that it does not suffer from the streaking effect known for example from standard dynamic programming [6]. The section concludes by introducing how to accumulate the cost on only half of the image domain without losing disparity resolution (in contrast to [2]). We simply refer to this as *Half-Resolution SGM*. The evaluation methodology is outlined in Section IV. We present four real-world sequences, each of 400 trinocular stereo frames. A quality measure, based on a trinocular stereo evaluation methodology [7], is used to quantify the relative performance of different accumulation strategies. Additionally we evaluate SGM on 396 stereo pairs for which sub-pixel accurate ground truth is available. The results of this study are presented and discussed in Section V. They suggest that path reduction is a very good option to gain significant run-time speed-ups. All findings of this study are summarized in Section VI.

The first author thanks the German Academic Exchange Service (DAAD) for financial support.

II. SEMI-GLOBAL MATCHING

This section gives a formal outline of the integration step of the SGM algorithm [1], as we mainly focus on this part of the method.

We introduce the notation for defining the cost accumulation procedure. For a cost accumulation path $L_{\mathbf{a}}$ with direction \mathbf{a} , processed between image border and pixel p , we consider the segment p_0, p_1, \dots, p_n of that path, with p_0 on the image border, and $p_n = p$. The cost at pixel position p (for a disparity d) on the path $L_{\mathbf{a}}$ is recursively defined as follows, for $i = 1, 2, \dots, n$:

$$L_{\mathbf{a}}(p_i, d) = C(p_i, d) + \mathcal{M}_i - \min_{\Delta} L_{\mathbf{a}}(p_{i-1}, \Delta) \quad (1)$$

with

$$\mathcal{M}_i = \min \left\{ \begin{array}{l} L_{\mathbf{a}}(p_{i-1}, d) \\ L_{\mathbf{a}}(p_{i-1}, d-1) + c_1 \\ L_{\mathbf{a}}(p_{i-1}, d+1) + c_1 \\ \min_{\Delta} L_{\mathbf{a}}(p_{i-1}, \Delta) + c_2(p_i) \end{array} \right\} \quad (2)$$

where $C(p, d)$ is the similarity cost of pixel p for disparity d , and c_1 and c_2 are the penalties of the smoothness term. The second penalty c_2 is individually adjusted at each pixel to $c_2(p_i)$. The magnitude of the forward difference in direction \mathbf{a} scales the penalty for each p_i with

$$c_2(p_i) := \frac{c_2}{|I(p_{i-1}) - I(p_i)|} \quad (3)$$

where $I(\cdot)$ refers to the intensity at a pixel. The reference configuration of the algorithm uses eight paths (up, down, left, right, and the in-between angles) for accumulation. To enforce uniqueness, two disparity maps are calculated to perform a left-right consistency check. A disparity passes this test if corresponding disparities do not deviate by more than one disparity level. The penalties are set to $c_1 = 30$ and $c_2 = 150$, for an intensity domain of $[0, 255]$. As similarity cost we employ the census cost which is defined in the next section. Several studies [8], [9] found this function to be very descriptive and robust, even under strong illumination variations, which is crucial for real-world applications.

A. Census Cost Function

The census transform [10] assigns to each pixel in the left and right image a signature vector, which is stored as bit string in an integer. This transformation is performed once prior cost calculation and signatures are stored in an integer matrix of the dimension of the image. The signature sequence is generated as follows

$$\text{census}_{\text{sig}} = \left[\Psi(I_{i,j} \geq I_{i+x,j+y}) \right]_{(x,y) \in \mathcal{N}} \quad (4)$$

where $\Psi(\cdot)$ returns 1 if true, and 0 otherwise. \mathcal{N} denotes a neighbourhood centred at the origin.

The census cost is the Hamming distance of two signature vectors and can be calculated very efficiently [12]. In fact, the cost of calculating the Hamming distance is proportional to the actual Hamming distance and not to the length of the signature string. This may become useful in GPU implementations when calculating the cost from scratch could

be cheaper than accessing global memory [3]. We employ a 9×3 window as we are working on a 32 bit machine and favour a stronger data contribution along the epipolar line.

III. INTEGRATION STRATEGIES

This section recalls the benefits of multiple paths minimization, which is the main reason for the great success of SGM. It also introduces different accumulation strategies which are evaluated according to the methodology as outlined in Section IV.

We use an example frame of a driving sequence that illustrates the following discussion. The left image of Figure 1 shows the result of the reference SGM algorithm when energy minimization is performed only along the epipolar line (here from left to right). This closely corresponds to

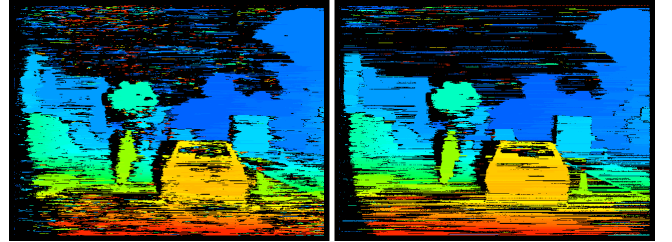


Fig. 1. Result of one horizontal accumulation path (left) and two horizontal paths (right).

the standard dynamic programming approach [6]. The right image shows when a second path (right to left) is minimized and results of the cost paths are accumulated. In both images the so called *streaking effect* is apparent, which is a result when cost paths are individually minimized without considering neighbouring image rows. Furthermore, objects seem to be slightly shifted along the accumulation direction when SGM is run with only one path. Introducing a second path that runs in opposite direction resolves this spatial bias. However, it can only slightly resolve the streaking effect. SGM suppresses the streaking effect by introducing non-horizontal cost accumulation paths which contribute to the final costs. Figure 2 shows on the left the improvement when two vertical integration paths are added. The right image of Figure 2 shows the result for 8-path accumulation (adding four diagonal directions). From visual inspection of this example we may conclude that the performance gain

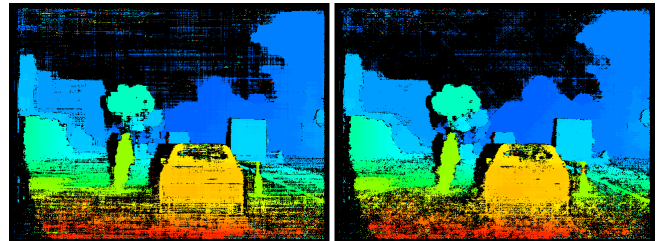


Fig. 2. Result of 4-path integration (left) and 8-path integration (right).

from two to four paths is significant, since the streaking effect is resolved by introducing vertical accumulation directions.

The benefit from four to eight paths, however, appears to be marginal only. This observation coincides with the study [5]. The next section introduces a 2-path accumulation strategy whose design pays special attention to resolve the streaking effect.

A. 2-Path Integration Strategies

The last section highlighted the streaking effect that results from horizontal 2-path integration. Adding non-horizontal paths solves this problem. The solution for removing the streaking comes from the fact that costs are accumulated also along vertical directions, propagating similarity information from neighbouring image rows across the image. So the question arises whether two paths could be sufficient to gain similar results as four paths, by choosing one vertical and one horizontal direction only and therefore also minimizing the energy semi-globally. We can think of two options to

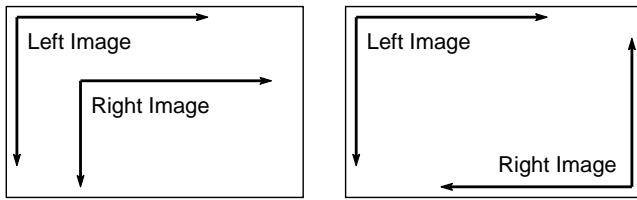


Fig. 3. 2-path integration strategies. Left: Identical setup. Right: Opposite setup.

apply semi-global 2-path integration strategies. First, we may choose for left and right disparity maps identical paths (e.g. down and right). However, as in case of one direction, this may result in a spatial bias along the chosen directions, such that disparities are slightly propagated across depth discontinuities and objects could be slightly displaced.

Another approach to resolve this potential problem is to use opposite path directions for left and right images. The intuition is that potential blur is discarded during the left-right consistency check. Figure 3 sketches both 2-path strategies. Results with those strategies are shown in Figure 4.

By comparing the results we notice that the opposite 2-path strategy lacks a certain amount of denseness. However, we see that this appears only to be true on low textured areas such as the road and along object boundaries. This effect may

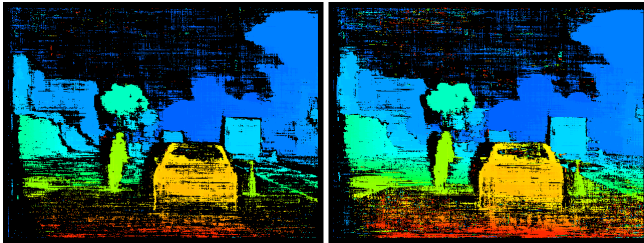


Fig. 4. Result of 2-path integration strategies. Left: Disjoint directions. Right: Identical directions.

become of benefit for the application of object segmentation in stereo images.

B. Half-Resolution SGM

Another idea to save resources is to apply the integration step, for example, only on even pixel indices, i.e. we perform the smoothness operation only on every second pixel of the image. The question is what happens with odd indices. There are two possible solutions. First we simply copy the cost at p_{2i} to p_{2i-1} . Thus all pixels at odd indices get a cost contribution from their left and right neighbouring pixel (as costs are passed back once for each direction). Figure 5 illustrates this strategy. Formally we change the definition

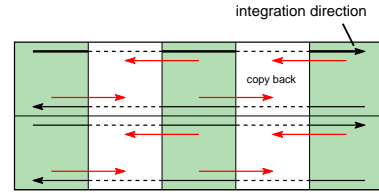


Fig. 5. Example of accumulation step showing two image rows. Calculated costs are passed back to neighbouring pixels.

of the accumulation path as follows:

$$L_{\mathbf{a}}(p_{2i}, d) = C(p_{2i}, d) + \mathcal{M}_{2i} - \min_{\Delta} L_{\mathbf{a}}(p_{i-1}, \Delta) \quad (5)$$

with

$$\mathcal{M}_{2i} = \min \left\{ \begin{array}{l} L_{\mathbf{a}}(p_{2i-2}, d) \\ L_{\mathbf{a}}(p_{2i-2}, d-1) + c_1 \\ L_{\mathbf{a}}(p_{2i-2}, d+1) + c_1 \\ \min_{\Delta} L_{\mathbf{a}}(p_{2i-2}, \Delta) + c_2(p_{2i}) \end{array} \right\} \quad (6)$$

and

$$L_{\mathbf{a}}(p_{2i-1}, d) = L_{\mathbf{a}}(p_{2i}, d) \quad (7)$$

In this study, this approach is applied only on 4-path SGM accumulation using the census cost function. There is no particular reason why half-resolution SGM was left out for 8-paths or even 2-paths, other than the way this approach evolved and was developed. However, the copy operation has a major contribution to the actual runtime, such that the performance gain is less than expected. Another option is to omit the copy operation. The disparity map will become more sparse. However, since this sparseness is evenly distributed over the whole image it will ultimately depend on the application whether this stereo map is sufficient for the anticipated purpose. In [2] SGM is run on down scaled image pairs to create a disparity overview. A second full resolution SGM is performed on a selected ROI to increase resolution for distant objects. Note, that the half-resolution approach presented here yields the opportunity to employ their approach but keep the resolution of the disparity, while accumulating only over half of the image domain. Thus, it may be possible to save a second full resolution SGM. A qualitative comparison in stereo performance and run-time would be of interest. Figure 6 shows the difference between

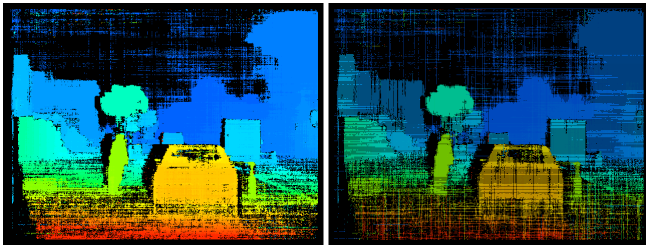


Fig. 6. Left: Half-resolution SGM. Right: Also omitting the copy operation.

regular 4-path half-resolution SGM with (left) and without (right) copy operation. In this evaluation the version with the copy operation is used.

IV. EVALUATION METHODOLOGY AND DATASETS

The different accumulation strategies as presented in Section III are evaluated on four real-world traffic sequences. Each of these sequences consist of 400 frames and shows typical urban environments. A trinocular stereo evaluation-based approach [7] is employed to quantify the quality of the generated stereo maps. To further support the obtained results of this evaluation we also tested the strategies on stereo data with available ground truth. Results from both methodologies are non-contradicting and support each other.

A. Real-World Data Sets

The data sets used in this evaluation have the names Queen Street, People, Harbour Bridge, Harbour Barriers and are available online [13]. They include many challenging scenes with several objects at different distances. Figure 7 shows the left frame of a stereo pair from the Queen Street sequence. On the right are corresponding disparity maps, generated by the half-resolution SGM approach.

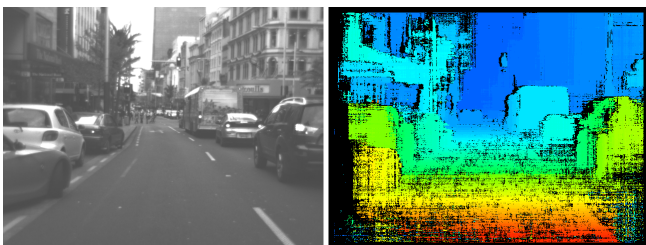


Fig. 7. Frame 75 from the Queen Street sequence with stereo map from half-resolution SGM.

1) *Trinocular Stereo Evaluation*: The prediction error technique of [7] for stereo sequences requires at least three different images of the same scene (from different perspectives at the same time instance). The objective is to generate a *virtual image* V from the output of a stereo matching algorithm, and to compare this with an image recorded by an additional *control camera*, that was not used to generate the disparity map. We generate the virtual image by mapping (warping) each pixel of the reference image into the position

in which it would be located in the *control image* N (i.e., the image recorded with the control camera). Then, N and V are compared by calculating the *normalized cross-correlation* (NCC) index between them as follows:

$$NCC(N, V) = \frac{1}{|\Omega|} \sum_{(i,j) \in \Omega} \frac{[N(i,j) - \mu_N][V(i,j) - \mu_V]}{\sigma_N \sigma_V} \quad (8)$$

where μ_N and μ_V denote the means, and σ_N and σ_V the standard deviations of the control and virtual images, respectively. The domain Ω is only for non-occluded pixels (i.e., pixels visible in all three images).

However, there is one significant bias in this measure. Inside textureless regions (e.g. the road area), incorrectly calculated disparities will not affect severely enough the final evaluation index if mapped into a wrong position inside the same textureless area. Therefore a mask is generated to reduce the domain Ω by leaving out textureless regions. The mask is produced in two steps. First, a *binarized gradient image* ∇I is calculated. This image is used to generate a Euclidean distance transformation [11] image I_d . We finally get the mask I_m as

$$I_m(i, j) = \begin{cases} 0 & \text{if } I_d(i, j) > T \\ 1 & \text{otherwise} \end{cases} \quad (9)$$

where T is a predefined threshold. The intuition is as follows. Miscalculated disparities at and within a certain distance around pixels with significant gradient (texture), should affect the index more than miscalculated disparities in textureless regions. Textureless regions as defined by the generated mask are discarded from the evaluation.

This approach may not solve the problem entirely but should result in a fairer comparison. However, trinocular stereo evaluation is in general a way to generate quantitative, and meaningful results that correlate well with subjective visual evaluations.

2) *Methodology*: We focus particularly on

- 1) The performance difference between 4- and 8-path integration. This is probably the most interesting evaluation because of the significant performance gain that comes with 4-path integration.
- 2) Performance difference between regular 4-path integration and half-resolution SGM over four paths.
- 3) To complete the evaluation both presented 2-path strategies are compared with each other and with the regular 4-path integration strategy which serves as reference performance.

B. Synthetic or Engineered Test Data

Synthetic or engineered stereo images provide a way to obtain ground truth, but come with their specifics [14]. We use a synthetic driving sequence [13] of 396 frames with available ground truth and refer to it as `Synthetic` sequence. This sequence was generated using computer graphic techniques [15] and provides sub-pixel accurate resolution in the ground truth image. This data set is used for the evaluation of the



Fig. 8. Frame 215 of the *Synthetic* sequence

accuracy of sub-pixel interpolation when applying different accumulation strategies.

1) *Sub-pixel Accuracy Evaluation*: In our sub-pixel evaluation we compare sub-pixel interpolation when performed on integrated costs. Because of the absence of noise and ideal lighting conditions in the *Synthetic* sequence, stereo matching is an easy task and we will get a dense disparity map of valid disparities. Here we consider a disparity value d_{opt} (at integer level) to be *valid* if $d_{opt} > 0$ and $|d_{opt} - d_{true}| < 0.5$, where d_{true} denotes the accurate disparity at the pixel location, which is available in high precision and d_{opt} is the disparity level with the minimum cost.

The nature of sub-pixel interpolation only allows a maximal disparity shift of $\delta_s < 0.5$. This however means that only if we calculate the sub-pixel displacement δ_s at pixels with valid disparities, can the disparity error be 0 (but also larger than 0.5), or formally $0 \leq |(d_{opt} + \delta_s) - d_{true}| < 1.0$. Our analysis follows following steps. For each image, first all valid disparities are identified by performing stereo matching without sub-pixel accuracy and the absolute error in disparity levels is calculated. Then the evaluation is repeated with sub-pixel accuracy interpolation at all valid disparities using the equiangular interpolation method [16] and the absolute error in disparity levels is calculated. We perform three evaluations of SGM with different accumulation strategies, namely 8-path, 4-path and half-resolution SGM. The results are accumulated in one histogram that display the average disparity error over all 396 frames. The results are normalized over the disparity density.

V. RESULTS AND DISCUSSION

We mainly focus on the comparison of performance results obtained from the trinocular stereo evaluation approach. Figure 9 shows the result of the *Queen Street* sequence. It was chosen because it has the largest differences between accumulation strategies from all sequences and can therefore serve as baseline result.

From the left chart in Figure 9 we see that index-curves of 4- and 8-path SGM follow exactly the same pattern, which indicates that both algorithm setups behave almost identical to different complexities and challenges in the stereo data. A frame with a significant index decrease in the 8-path setup results always in a similar decrease in the 4-path setup. There are no exceptions or contradicting tendencies. The

only difference is a small decrease of the index level when reducing 8- down to 4-paths.

These differences are everywhere less than 5% points, and most of the time only within 1 or 2% points. For the *Queen Street* sequence we observe a 2-3% decrease on an index level of 75% and higher. This yields a performance decrease of 4% maximum, but a significant run-time improvement during the expensive accumulation step of the algorithm. Of course, to ultimately quantify the performance loss, an extensive study on real-world sequences with approximate ground truth (e.g. generated by data from a LIDAR system), needs to be performed. However, our results already show that differences in performance, due to different scene complexities, affect both 8- and 4-path in exactly the same way and almost to the same extend.

The performance difference between 4-path SGM and 4-path half-resolution SGM is only marginal. The results for the *Queen Street* sequence are shown in the middle chart of Figure 9. The index curve indicate identical, and in case of the *Harbour Bridge* sequence even superior performance for half-resolution SGM.

The almost identical performance can be explained by the used cost function and copy operation. The census cost function considers information of neighbouring pixels which includes the pixels omitted during the accumulation step. Also, since path costs (rather than just data costs) are copied from both neighbouring pixels along the current path, the cost at an omitted pixel also incorporates the SGM smoothness constraint.

Another possible option for this approach is to run SGM with two different cost functions that yield different characteristics or advantages. The first run, for example, could employ a cost function on even pixel indices, another run uses a different cost function on odd indices. The benefit of combining two data descriptors in this way instead of merging cost in the data term only, is that the smoothness constraint is already incorporated during the merge step. However, we consider this as an interesting option for future research.

The final evaluation considers the difference in performance between the two proposed 2-path integration strategies, and compares the performance with the SGM 4-path integration as reference. Figure 9 shows the results (right chart).

There is a significant difference of performance when comparing 2-path integration in opposite directions with 2 path integration that yield the same vertical and horizontal directions for left and right input frame. However, performance results are close when comparing the latter 2-path with the regular 4-path integration approach. The 4-path accumulation step however seems overall to slightly outperform the 2-path approach. Although the run-time performance of two path accumulation would be improved compared to the 4-path accumulation, the benefit would be marginal when compared to the run time of the 8-path accumulation setup. Nonetheless, the similar performance to 4 path integration is interesting. The weak result of the 2-path strategy using

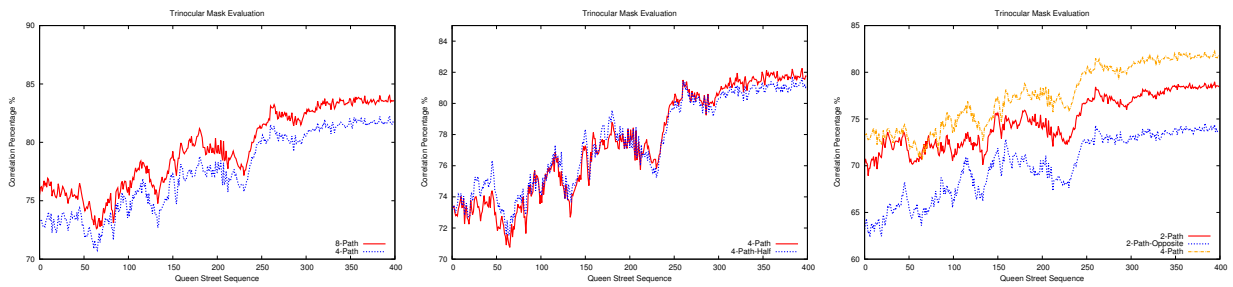


Fig. 9. Correlation percentage curves for the Queen Street sequence. Left: 4- versus 8-path SGM accumulation. Centre: 4-path standard versus 4-path half-resolution SGM. Right: both 2-path integration strategies.

opposite directions is likely due to the lower density of the stereo map.

The results from the sub-pixel evaluation in Figure 10 confirm the discussed results as well for sub-pixel calculations. It appears that 8-path SGM get slightly better result when looking at quantities of sub-pixel errors < 0.1 , but it also has a larger quantity of errors > 0.4 than the 4-path strategies.

Of course, running SGM on real-world traffic sequences with available ground truth ultimately shows how many paths yield which level of performance. Extensive traffic-scene data sets with available ground truth is unfortunately not available, yet. We used trinocular stereo evaluation for our analysis which gives an indication that reducing the accumulation paths will result in a stereo map with sufficient quality for subsequent applications. Ultimately this is what matters and can give an implicit quality measure: If an application can operate on a 4-path SGM stereo-map equally good as on a 8-path SGM stereo-map, 4-path integration should be considered in algorithm design to gain possible run-time improvements. The argument that processing power increases constantly is not excluding considerations for decreases in run-time; note that usually requirements of applications (e.g., recording speed or image resolution) also advance.

VI. CONCLUSIONS

We compared stereo performance of the SGM algorithm when using different accumulation strategies. Results indicate that, depending of the application, an insignificant reduction of quality can be tolerated in return for a significantly

faster execution. The study also introduced 2-path integration strategies in SGM that do not suffer from the streaking effect.

Furthermore, running SGM only on half of the resolution of the image (without losing disparity resolution) was proposed. Performance was almost identical to the regular 4-path SGM. This approach offers new ways for cost integration in a more general sense.

REFERENCES

- [1] H. Hirschmüller. Accurate and efficient stereo processing by semi-global matching and mutual information. In Proc. *Computer Vision Pattern Recognition*, volume 2, pages 807–814, 2005.
- [2] S. K. Gehrig, F. Eberli, and T. Meyer. A real-time low-power stereo vision engine using semi-global matching. In Proc. *Computer Vision Systems*, LNCS 5815, pages 134–143, 2009.
- [3] I. Ernst and H. Hirschmüller. Mutual information based semi-global stereo matching on the GPU. In Proc. *Int. Symp. Advances Visual Computing*, pages 228–239, 2008.
- [4] S. Hermann, R. Klette, and E. Destefanis. Inclusion of a second-order prior into semi-global matching. In Proc. *Pacific Rim Symp. Image Video Technology*, LNCS 5414, pages 633–644, 2009.
- [5] I. Haller, C. Pantillie, F. Oniga, and S. Nedevschi. Real-time semi-global dense stereo solution with improved sub-pixel accuracy. In Proc. *Intelligent Vehicles Symp.*, pages 369–376, 2010.
- [6] Y. Ohta and T. Kanade. Stereo by two-level dynamic programming. In Proc. *Int. Joint Conf. Artificial Intelligence*, pages 1120–1126, 1985.
- [7] S. Morales, T. Vaudrey, and R. Klette. A third eye for performance evaluation in stereo sequence analysis. In Proc. *Computer Analysis Images Patterns*, pages 1078–1086, 2009.
- [8] H. Hirschmüller and D. Scharstein. Evaluation of stereo matching costs on images with radiometric differences. *IEEE Trans. Pattern Analysis Machine Intelligence*, **31**:1582–1599, 2009.
- [9] S. Hermann, S. Morales, T. Vaudrey, and R. Klette. Illumination invariant cost functions in semi-global matching. In Proc. *Computer Vision Vehicle Technology: Earth to Mars*, ACCV workshop, to appear, 2011.
- [10] R. Zabih and J. Woodfill. Non-parametric local transform for computing visual correspondence. In Proc. *Europ. Conf. Computer Vision*, volume 2, pages 151–158, 1994.
- [11] T. Saito and J. Toriwaki. New algorithms for n-dimensional Euclidean distance transformation. *Pattern Recognition*, **27**:1551–1565, 1994.
- [12] P. Wegener. A technique for counting ones in a binary computer. *Comm. ACM*, **3**:322, 1960.
- [13] *.enpeda.. image sequences analysis test site. www.mi.auckland.ac.nz/EISATS*
- [14] R. Haeusler and R. Klette. Benchmarking stereo data (not the matching algorithms). In Proc. *DAGM*, LNCS 6376, pages 383–392, 2010.
- [15] T. Vaudrey, C. Rabe, R. Klette, and J. Milburn. Differences between stereo and motion behaviour on synthetic and real-world stereo sequences. In Proc. *Image Vision Computing New Zealand*, pages 1–6, 2008.
- [16] M. Shimizu and M. Okutomi. An analysis of subpixel estimation error on area-based image matching. In Proc. *Digital Signal Processing*, volume 2, pages 12391242, 2002.

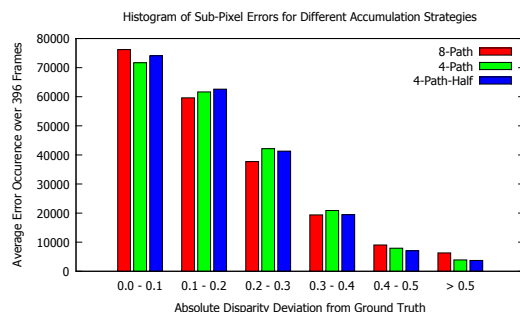


Fig. 10. Results of the sub-pixel accuracy evaluation.